Synthesis of Adaptive Polymer Brushes via "Grafting To" Approach from Melt

ARTICLE *in* LANGMUIR · JANUARY 2002

Impact Factor: 4.46 · DOI: 10.1021/la015637q

Synthesis of Adaptive Polymer Brushes via "Grafting To" Approach from Melt

Sergiy Minko,* Satish Patil, Vitaliy Datsyuk, Frank Simon, Klaus-Jochen Eichhorn, Michail Motornov, Denys Usov, Igor Tokarev, and Manfred Stamm

Department of Polymer Interfaces, Institut für Polymerforschung Dresden e.V., Hohe Strasse 6, 01069 Dresden, Germany

Received October 19, 2001

We report a simple method to synthesize binary polymer brushes from two incompatible polymers of different polarity. The synthetic route is based on a subsequent step-by-step grafting of carboxyl-terminated polystyrene and poly(2-vinylpyridine) to the surface of a Si wafer functionalized with 3-glycidoxypropyltrimethoxysilane. The end-functional polymers were spin-coated on the substrate, and grafting was carried out at a temperature higher than the glass transition temperature of the polymers. The composition of the binary brushes can be regulated based on grafting kinetics of the first polymer by the change of time or/and temperature of grafting. This method reveals a smooth and homogeneous polymer film on the macroscopic scale, while at the nanoscopic scale the system undergoes phase segregation effecting switching/adaptive properties of the film. Upon exposure to different solvents, the film morphology reversibly switches from "ripple" to "dimple" structures as well as the surface energetic state switches from hydrophobic to hydrophilic. The same switching of hydrophilic/hydrophobic properties was obtained for the different ratios between two grafted polymers in the binary brush.

Introduction

Grafting of polymers is a widely used method for the modification of solid surfaces. A number of grafting points per polymer chain can be different and affects properties of the grafted chains.[1] A thin film with polymer chains grafted to the solid substrate by only one end is a very suitable subject for theoretical analysis and experimental study, because its behavior can be easily modeled and interpreted.[2] If the distance between grafted chains is smaller than an average end-to-end distance of the polymer chain, the layer of the grafted chains is in the regime of the polymer brush. In this regime, grafted chains are forced to stretch in the direction normal to the plane of grafting and the conformation is determined by the energy balance between the elastic free energy of the stretched chain and the energy of the interaction between statistical segments.[3] Such an arrangement offers many interesting applications of the brushlike layers[4] that have stimulated great interest in synthesis and investigation of polymer brushes.[5] The questions of the regulation of thin polymer film stability,[6] wettability,[7] adhesion,[8] reactivity and cell protein interaction,[9] micro/nano-patterning,[10] swelling,[11] friction,[12] stabilization of colloids,[13] core−shell structures,[14] and so forth were addressed with respect to the employment of polymer brushes.

Here, we describe the synthesis of adaptive and switchable surfaces/thin polymer films fabricated from two incompatible carboxyl-terminated polymers chemically grafted to Si substrates. These two grafted polymers form the mixed (binary) brushlike layer. The theoretical analysis of phase segregation in binary brushes results in a complicated phase diagram[15] and plenty of the thin film morphologies.[16] Depending on solvent quality, layered and rippled phases, or their mixture, were observed experimentally. A transition between different morphologies upon external stimuli (solvent, temperature, etc.) results in switching of surface properties of the film, for example, from hydrophilic to hydrophobic or from smooth to rough.[17] Such surfaces partially mimic a cell membrane

* To whom correspondence should be addressed. Tel: +49 351-4658-271. Fax: +49 351-4658-284. E-mail: minko@ipfdd.de.

(1) Gong, L.; Friend, A. D.; Wool, R. P. *Macromolecules* **1998**, *31*, 3706−3714.

(2) Szeleofer, I.; Carigano, M. A. *Adv. Chem. Phys.* **1996**, *94*, 165−259.

(3) (a) Alexander S. J. *J. Phys (Paris)* **1977**, *38*, 983−987. (b) Milner, S. T. *Science* **1991**, *251*, 905−914.

(4) Halperin, A.; Tirrell, M.; Lodge, T. P. *Adv. Polym. Sci.* **1992**, *100*, 31−71.

(5) Thao, B.; Brittain, W. J. *Prog. Polym. Sci.* **2000**, *25*, 677−710 and references therein.

(6) Zerushalmi-Royen, R.; Klein, J.; Fetters, L. *Science* **1994**, *263*, 793−795.

(7) Mansky, P.; Liu, Y.; Huang, E.; Russell, T. P.; Hawker, C. J. *Science* **1997**, *275*, 1458−1460.

(8) (a) Raphael, E.; de Gennes, P. G. *J. Phys. Chem.* **1992**, *96*, 4002−4007. (b) Ruths, M.; Johannsmann, D.; Rühe, J.; Knoll, W. *Macromolecules*, **2000**, *33*, 3860−3870.

(9) (a) Aksay, A.; Trau, M.; Manne, S.; Honma, I.; Yao, N.; Zhou, L.; Fenter, P.; Eisenberger, P. M.; Gruner, S. M. *Science* **1996**, *273*, 892−894. (b) McPherson, T.; Kidane, A.; Szleifer, I.; Park, K. *Langmuir* **1998**, *14*, 176−186.

(10) Niu, Q. J.; Frechet, J. M. *Angew. Chem., Int. Ed. Engl.* **1998**, *37*, 667−670. (b) Husseman, M.; Benoit, D. G.; Frommer, J.; Mate, M.; Hinsberg, W. D.; Hendrick, J. L.; Hawker, C. J. *J. Am. Chem. Soc.* **2000**, *122*, 1844−1845.

(11) Habicht, J.; Schmidt, M.; Rühe, J.; Johannsmann, D. *Langmuir* **1999**, *15*, 2460−2465.

(12) (a) Klein, J.; Kumacheva, E.; Mahalu, D.; Perahia, D.; Fetters, L. J. *Nature* **1994**, *370*, 634−636. (b) Berman, A.; Steinberg, S.; Campbell, S.; Ulman, A.; Israelachvili, J. N. *Tribol. Lett.* **1998**, *4*, 43−48.

(13) Pincus, P. *Macromolecules* **1991**, *24*, 2912−2919.

(14) Guo, X.; Weiss, A.; Ballauff, M. *Macromolecules* **1999**, *32*, 6043−6046.

(15) (a) Marko, J. F.; Witten, T. A. *Phys. Rev. Lett.* **1991**, *66*, 1541−1546. (b) Lai, P.-Y.; Binder, K. *J. Chem. Phys.* **1992**, *97*, 586−595. (c) Lai, P.-Y. *J. Chem. Phys.* **1994**, *100*, 3351−3357. (d) Brown, G.; Chakrabarti, A.; Marko, J. F. *Europhys. Lett.* **1994**, *25*, 239−244. (e) Soga, K. G.; Zuckermann, M. J.; Guo, H. *Macromolecules* **1996**, *29*, 1998−2005.

(16) (a) Minko, S.; Sidorenko, A.; Goreshnik, E.; Usov, D.; Stamm, M. *Polym. Mater. Sci. Eng.* **2000**, *83*, 533−534. (b) Minko, S.; Stamm, M.; Goreshnik, E.; Usov, D.; Sidorenko, A. *Polym. Mater. Sci. Eng.* **2000**, *83*, 629−630.

10.1021/la015637q CCC: $22.00
Published on Web 01/02/2002

adaptive behavior and promise numerous interesting applications. These thin films can be considered as a new type of smart nanostructural materials. Recently the "grafting from" approach for synthesis of the smart polymer surfaces from binary polymer brushes[18] and block-copolymer brushes[19] was reported in the literature. This approach allows preparation of brushes with high grafting density from the chains of high molecular weight. Up to 50−100 nm (dry film) thick brushes can be synthesized by polymerization from the solid surface. Nevertheless, this approach has substantial disadvantages. First of all, it is a complicated synthesis involving a multistep procedure and requiring a high purity of the reaction mixture. Second, synthesis of polymers can be better controlled in solution as compared to the polymerization on the surface.[20] It is valid for almost all polymerization mechanisms. Consequently, there are clear reasons to develop alternative methods for synthesis of mixed brushes from end-terminated polymers prepared under very well controlled conditions (e.g., anionic polymerization).

Experimental Section

Materials. Carboxyl-terminated polystyrene (PS16K−COOH; M_n = 16 900 g/mol, M_w = 21 900 g/mol) synthesized by atom free living polymerization using 4-(1-bromoethyl)benzoic acid as initiator and maleic anhydride terminated polypropylene (PP−MA; M_n = 24 000 g/mol, M_w = 62 000) were kindly offered by Dr. J. Pionteck. PS−COOH of other molecular weights, PS2K−COOH (M_n = 2000 g/mol, M_w = 2980 g/mol), PS45K−COOH (M_n = 45 900 g/mol, M_w = 48 400 g/mol), PS70K−COOH (M_n = 72 300 g/mol, M_w = 75 200 g/mol), PS670K−COOH (M_n = 672 000 g/mol, M_w = 709 000 g/mol), and poly(2-vinyl pyridine) (PVP−COOH; M_n = 39 200 g/mol, M_w = 41 500 g/mol), were purchased from Polymer Source, Inc. (synthesized by anionic polymerization). Toluene and tetrahydrofuran (THF) were distilled after drying over sodium. Dichloromethane was dried on molecular sieves. Highly polished silicon wafers (obtained from Wacker-Chemitronics) were first cleaned in an ultrasonic bath for 30 min with dichloromethane, placed in cleaning solution (prepared from NH_4OH and H_2O_2) at 60 °C for 1 h, and then rinsed several times with Millipore water (18 MΩ cm^{-1}). 3-Glycidoxypropyl trimethoxysilane (GPS) ABCR (Karlsruhe, Germany) was used as received.

Preparation of the Binary Brushes. In our route of synthesis, we explore the method of grafting of an end-terminated polymer from the melt recently reported by I. Luzinov et al.[21] GPS was chemisorbed on the surface of the cleaned Si wafers from 1% solution in the dried toluene for 16 h at room temperature. Afterward, the reaction samples were carefully rinsed with toluene and ethanol to remove ungrafted GPS.

In the next step, a thin film (50 ± 5 nm as measured with ellipsometry) of PS−COOH was spin-coated on the top of the GPS layer from the 1% toluene solution. Then the film was heated at 150 °C in a vacuum oven for different periods of time to graft PS−COOH and to measure the kinetics of grafting. The non-grafted polymer was removed by Soxhlet extraction with toluene for 5−7 h. Then the second polymer, PVP−COOH, was spin-coated on top of the film and the heating procedure followed by subsequent Soxhlet extraction to remove any ungrafted polymer was performed.

Each step was monitored with ellipsometry, atomic force microscopy (AFM), and X-ray reflectivity measurements. The same procedure was performed on the surface of a silicon prism and monitored with Fourier transform infrared spectroscopy with attenuated total reflection (FTIR-ATR).

Control experiments showed that PS−COOH deposited on the bare Si wafer was completely removed by Soxhlet extraction with THF, while PVP−COOH left the small amount of 0.5 mg/m² of the adsorbed polymer.

Table 1. Comparison of the Thin Film Characteristics Obtained from Ellipsometry, AFM, and X-ray Reflectivity Experiments

	thickness, nm		rms, nm	
layer	ellipsometry	X-ray	AFM	X-ray
GPS	1.5	1.7	0.2−2.2[a]	0.42
grafted PS−COOH	5.5	5.6	0.40	0.47
binary brush	7.5	7.5	0.71	0.75

[a] rms differs strongly on areas contaminated with polyGPS particles.

Sample Characterization. *Ellipsometry*. Layer thickness and grafted amounts were evaluated at λ = 633 nm and an angle of incidence of 70° with a Multiscope Optrel (Berlin, Germany) null-ellipsometer equipped with an *XY*-positioning table for mapping of the sample surface (lateral resolution is defined by the beam spot of about 2 mm). The measurements were performed for each sample after each step of the modification to use the measurements of the previous step as a reference for the simulation of ellipsometric data. Initially, the thickness of the native SiO_2 layer (usually 14 ± 2 Å) was calculated at refractive indexes N = 3.858-i0.018 for the Si substrate and n = 1.4598 for the SiO_2 layer. The thickness of the GPS layer (typically 14 ± 3 Å) was evaluated using the two-layer model: SiO_2/GPS for a refractive index of GPS equal to 1.429. The thickness of PS−COOH or PVP−COOH as the first grafted layer (typically 1−7 nm) was evaluated with the three-layer model SiO_2/GPS/PS−COOH with n = 1.59 or in the case of SiO_2/GPS/PVP−COOH, n = 1.595. Finally, the thickness of the whole polymer film (typically 5−8 nm) after grafting of the second polymer (for example, PVP−COOH) was calculated using the three-layer model SiO_2/GPS/polymer considering the thin polymer film as an effective optical medium with n = 1.59. From the obtained values, we calculated the grafting amount of each polymer $A = H\rho$, and the grafting density $\Sigma = AN_A/M_w$ where H is the ellipsometric thickness, ρ is the density, N_A is Avogadro's number, and M_w is the molecular weight. The morphology of the phase-segregated film and the roughness of the film change upon exposure to different solvents. Nevertheless, that does not affect ellipsometric data, because of the small difference between the refractive indexes of PS and PVP. The results of ellipsometric measurements agree very well with the thickness of each layer evaluated from the simulation of X-ray reflectivity data (Table 1).

X-ray Photoelectron Spectroscopy (XPS). XPS experiments were performed with an AXIS ULTRA spectrometer (Kratos Analytical, U.K.) equipped with a monochromized Al Kα X-ray source of 300 W at 20 mA. The analyzer's pass energy was set to 160 eV to record survey spectra and 20 eV to take high-resolution spectra. Spectra were recorded for the four samples: S1, Si wafer with chemisorbed GPS; S2, the same sample after labeling of the epoxy groups with *n*-butylamine; S3, the S1 sample with grafted PS−COOH; and S4, the S3 sample labeled with *n*-butylamine to evaluate the amount of residual epoxy groups.

All spectra were charge compensated using the C_xH_y component peak of the C 1s spectra at BE = 285.00 eV (for the samples S1 and S2) and BE = 284.76 eV (for the samples S3 and S4) as reference peaks. To determine elemental ratios, normalized peak areas were calculated from peak areas of survey spectra, respecting experimentally determined sensitivity factors and the spectrometer's transmission function.

FTIR-ATR. FTIR-ATR spectra were taken with an IFS 55 (Bruker) spectrometer for the chemisorbed GPS layer, grafted PS−COOH, grafted PVP−COOH layers, and the binary PS/PVP

(17) Minko, S.; Usov, D.; Goreshnik, E.; Stamm, M. *Macromol. Rapid Commun.* **2001**, *22*, 206−211.

(18) Sidorenko, A.; Minko, S.; Schenk-Meuser, K.; Duschner, H.; Stamm, M. *Langmuir* **1999**, *15*, 8349−8355.

(19) (a) Zhao, B.; Brittain, W. J. *J. Am. Chem. Soc.* **1995**, *117*, 3557−3558. (b) Sedjo, R. A.; Mirous, B. K.; Brittain, W. J. *Macromolecules* **2000**, *33*, 1492−1493.

(20) (a) Minko, S.; Gafiychuk, G.; Sidorenko, A.; Voronov, S. *Macromolecules* **1999**, *32*, 4525−4531. (b) Minko, S.; Sidorenko, A.; Stamm, M.; Gafijchuk, G.; Senkovsky, V.; Voronov, S. *Macromolecules* **1999**, *32*, 4532−4538.

(21) (a) Luzinov, I.; Julthongpiput, D.; Malz, H.; Pionteck, J.; Tsukruk, V. V. *Macromolecules* **2000**, *33*, 1043−1048. (b) Tsukruk, V. V.; Luzinov, I.; Julthongpiput, D. *Langmuir*, **1999**, *15*, 3029−3032. (c) Luzinov, I.; Julthongpiput, D.; Liebmann-Vinson, A.; Cregger, T.; Foster, M. D.; Tsukruk, V. *Langmuir* **2000**, *16*, 504−516.

Scheme 1. Schematic Representation of the Synthesis of Binary Brushes[a]

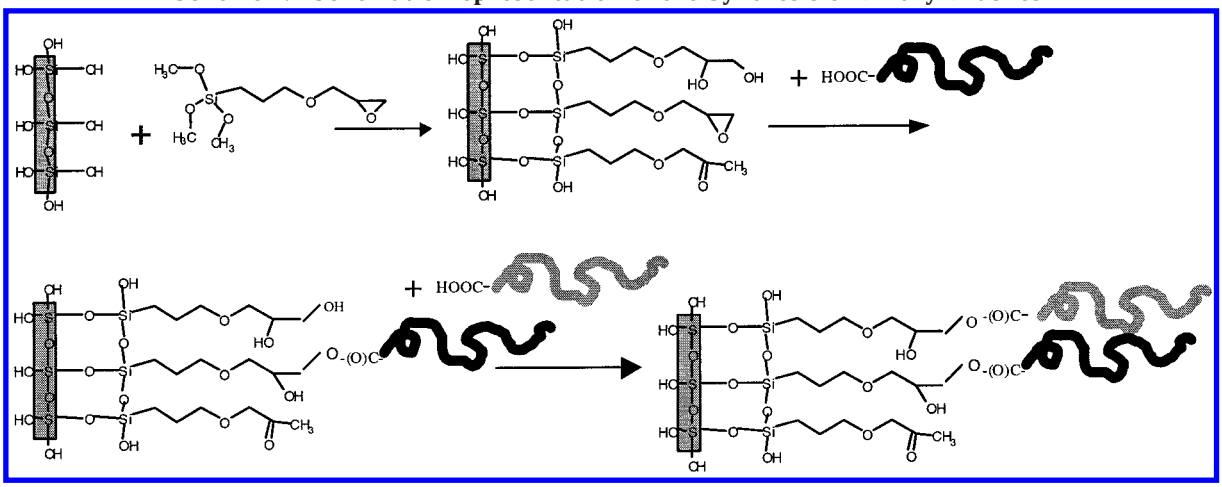

[a] PS chains, black; PVP chains, gray. The GPS grafted layer offers many different functionalities (attachment to the surface via epoxy groups and oxidation of epoxy groups is not shown in the scheme).

grafted layers using the Si prism with a native SiO_2 layer as a substrate for the grafting.

AFM. AFM studies were performed on a Dimension 3100 (Digital Instruments, Inc., Santa Barbara, CA) microscope. The tapping and phase modes were used to map the film morphology at ambient conditions. Silicon tips with a spring constant of 1.5−6.3 N/m and a frequency of 63−100 kHz were used. Root mean square roughness (rms) and power spectra density (PDS) of the images were evaluated using the commercial software (Table 1).

X-ray Reflectivity. X-ray reflectivity measurements were performed with a diffractometer XRD 3003 T/T (Seifert FPM, Germany) (λ = 1.54 Å) operated in reflectivity mode. The experimental data were analyzed by simulation of the reflectivity curves based on Parratt's formalism using the step shape layered model.[22] The interface roughness was introduced as a transition interlayer with an electron density profile described by an error function.

Contact Angle. The advancing contact angle of water was measured using DSA Krüss (Hamburg, Germany) equipment.

Results and Discussion

Grafting of GPS. Our synthetic procedure (Scheme 1) starts with the covalent grafting of GPS to the surface of a Si wafer as mentioned in the experimental part. For such conditions, it is possible to approach a reproducible preparation of covalently bonded thin layers of GPS. AFM topographical images of the surface covered with GPS (Figure 1) showed only few clusters of polymerized and precipitated GPS (typical spots of 20−100 nm in diameter and of 1−3 nm height), which do not have an influence on the following investigations. The amount of these poly-GPS particles usually decreases after the subsequent procedure of grafting of polymers. Consequently, many particles are not strongly adhered to the substrate. The ellipsometric thickness of the films of about 14 ± 3 Å corresponds to the 1−1.5 theoretical monolayers of the GPS.[21] This is evidence of a complicated structure of the GPS layers resulting from parallel chemical reactions of methoxysilane fragments, hydrolyzed by traces of water, with surface Si−OH groups and with silanol groups of neighboring GPS molecules. Nevertheless, the film is macroscopically uniform as was obtained from the mapping of the wafer using ellipsometry (Figure 2). The average surface concentration of GPS calculated from ellipsometry data is in the range of 4 molecule nm^{-2}.

XPS data for the chemisorbed GPS on the surface of the Si wafer are shown in Figure 3. The C 1s spectrum was

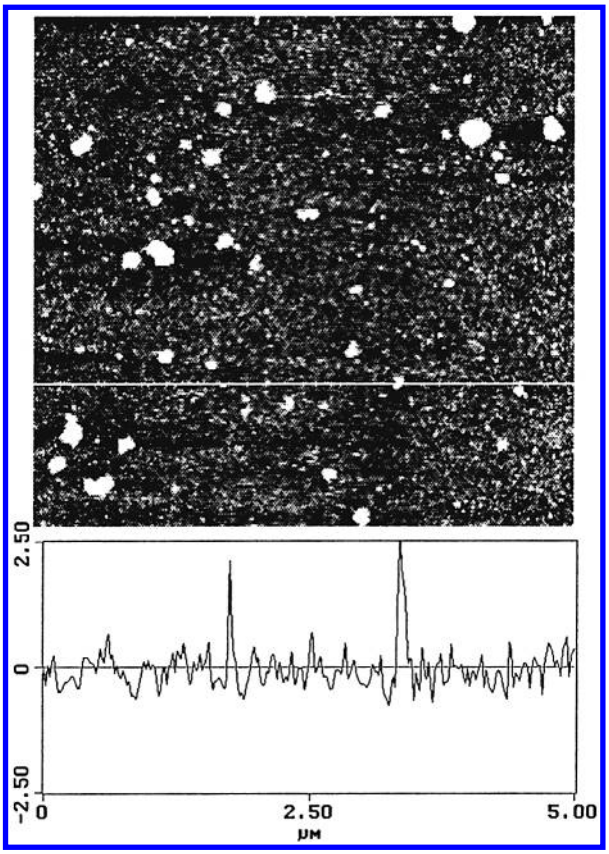

Figure 1. AFM topography image and corresponding cross section of chemisorbed GPS on a Si wafer (*Z*-axis in nm). The bumps represent contamination originated from particles of polymerized GPS.

decomposed into five component peaks named A, B, C, D, and E. According to their binding energies, different carbon species may be distinguished[23] as presented in Table 2. The areas of the two component peaks B and E are equal, because their stoichiometric ratio is [B]/[E] = 1:1. The binding energy found for peak D is somewhat larger than that reported in the literature (287.02 eV). The XPS data show that grafted GPS contains only a small fraction of epoxy groups. Most of them have undergone a ring-opening

(22) Tolan, M. *X-ray scattering from soft-matter thin films*; Springer: Berlin, 1999; Chapter 2.3.

(23) Beamson, G.; Briggs, D. *High resolution of organic polymers, The Scienta ESCA 300 Database*; J. Wiley & Sons: New York, 1992; p 26.

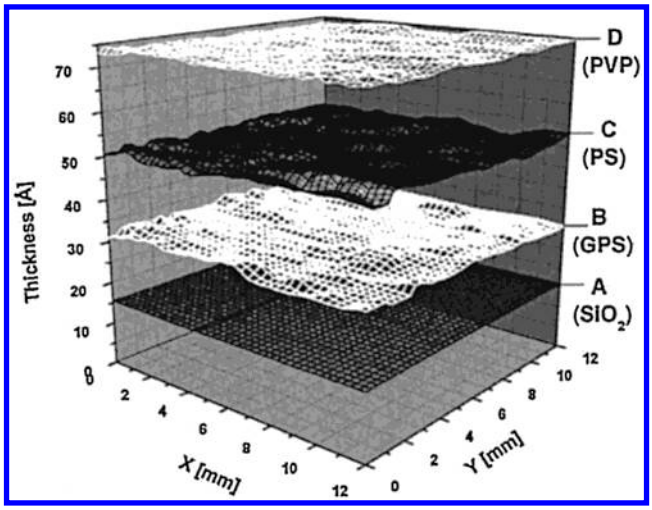

Figure 2. Ellipsometric mapping of the surface of a Si wafer followed each step of grafting. The *Z*-axis represents the increasing layer thickness starting from the Si substrate (zero point): SiO_2 native layer after cleaning (A), grafted GPS (B), grafted PS16K−COOH (C), grafted binary brush PS16K−COOH + PVP−COOH (D).

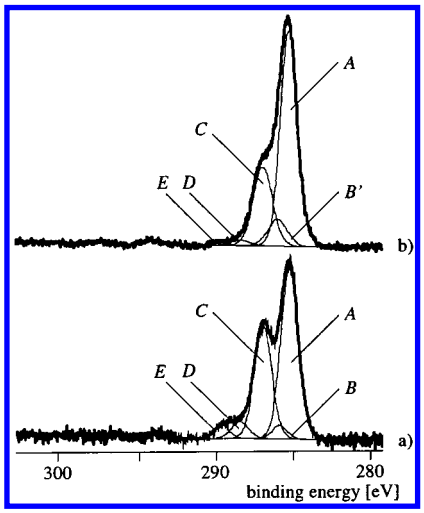

Figure 3. C 1s high-resolution X-ray photoelectron spectra of GPS grafted onto a silicon wafer before (a) and after labeling with *n*-butylamine (b) (A = C_xH_y; B = −C−C(O)OR; B′ = −C−N; C = −C−OH and −C−O−C−; D = epoxy groups; E = −O−C═O).

reaction and isomerization to carbonyl groups or even oxidation (the latter can be assumed from the component peaks B and E). This conclusion was proved by labeling of residual epoxy groups of the grafted GPS with *n*-butylamine. In the C 1s spectrum (Figure 3b), component peaks D and E have nearly disappeared. Component peak B′ is significantly increased. This indicates the reaction of *n*-butylamine with residual epoxide rings forming secondary amines (C−NH−C). The peak B′ represents those amino bonds. According to the above-mentioned reaction between amine and epoxy groups, the ratio [N]/[C] was determined from the C 1s spectrum to be

$$\frac{[N]}{\Sigma carbons} = \frac{0.5\,[B']}{[A] + [B'] + [C] + [D] + [E]} = 0.0408$$

The value found is in excellent agreement with the ratio [N]/[C] = 0.0407 obtained from the survey spectrum. Component peak C shows the presence of *C*−OH and *C*−O−*C* bonds. The small component peak D indicates epoxy groups which were not involved in the labeling reaction.

Table 2. Component Peaks of C 1s XPS for Chemisorbed GPS

A	B	C	D	E
285.000 eV	285.673 eV	286.723 eV	288.207 eV	289.374 eV
C_xH_y	β-shift of E *C*−COO	−*C*−O *C*−OH	C in epoxy group	O═*C*−O[a]

[a] Probably carbonic acids (−*C*OOH).

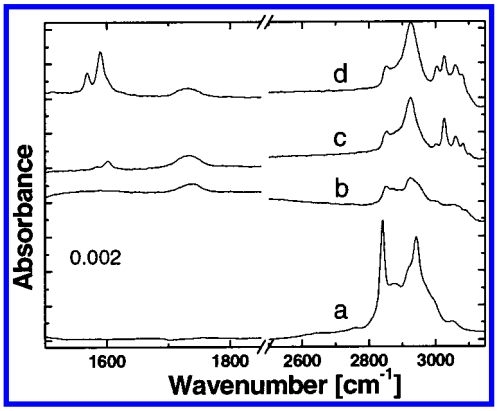

Figure 4. FTIR-ATR spectra: (a) thin GPS film (reference), (b) chemisorbed GPS, (c) PS16K−COOH brush, and (d) PS16K−COOH and P2CVP−COOH mixed brush.

The same procedure to chemisorb GPS was performed on the surface of a silicon prism. The FTIR-ATR spectrum also identifies characteristic bands of GPS on the surface (Figure 4b). As a reference, we used the spectrum of a liquid GPS film deposited on the prism (Figure 4a). Here, we present FTIR-ATR spectra for the 1500−3200 cm^{-1} wavenumber range. The characteristic bands of epoxy groups (736−854, 863−950, and 1260 cm^{-1}) could not be detected in the very thin layer of grafted GPS. We can only identify the hydrocarbon bands (C−H stretching vibrations) at 2800−3100 cm^{-1} which are similar for both spectra (Figure 4a,b). In contrast to the nongrafted GPS in the chemisorbed layer, the methoxy band (2842 cm^{-1}) decreases, as expected, and a very pronounced carbonyl band at 1740 cm^{-1} appears. In this respect, FTIR and XPS data are in good correlation showing carbonyl compounds in the grafted GPS layer. The appearance of carbonyl compounds at the GPS/silica interface was already discussed in the literature.[24]

The scenario of GPS chemisorption involves not only hydrolysis and reaction of trimethoxysilane groups with surface silanol groups but additionally opening of the epoxy ring of GPS. Epoxy groups are able to react directly with silanol groups forming Si−O−C bonds[25] and OH groups in the β position which can initiate new ring-opening reactions. Hydrolysis of epoxy rings by traces of water also produces −OH functionalities initiating further ring-opening reactions. In addition, vicinal diols formed in the reaction of hydrolysis of epoxy groups possess isomerization or oxidation to carbonyl compounds. Estimations using XPS data show that about 5−10% of GPS molecules still have epoxy functionality in the chemisorbed layer and about the same amount are oxidized to form carbonyl compounds. The residual fraction of GPS molecules form vicinal diols or bond directly to the substrate via Si−O−C bonds. Consequently, the chemisorbed GPS forms the layer

(24) (a) Horr, T. J.; Ralston, J.; Smart, R. St. *Colloids Surf.* **1992**, *63*, 21−28. (b) Horr, T. J.; Reynolds, G. D. *J. Adhes. Sci. Technol.* **1997**, *11*, 995−1009.

(25) (a) Heublein, G.; Heublein, B.; Hortschansky, P.; Schütz, H.; Flammerscheim, H. J. *Macromol. Chem.* **1989**, *190*, 9−18. (b) Heublein, G.; Taeger, F. *Acta Polym.* **1988**, *39*, 701−704.

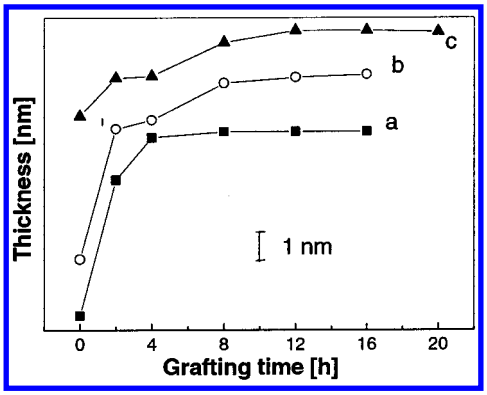

Figure 5. Grafting kinetics of polymer brushes: (a) PS16K−COOH, (b) PVP−COOH, and (c) PVP−COOH on the wafer with grafted PS16K−COOH (initial thickness 3.5 nm).

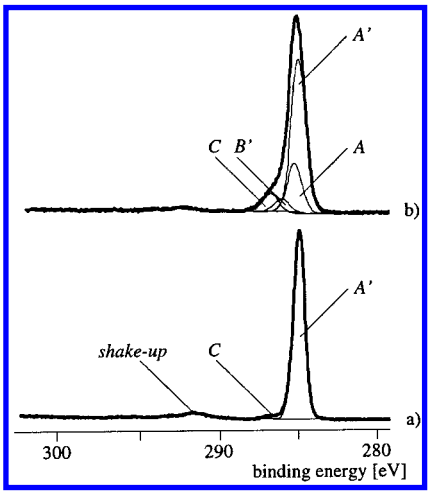

Figure 6. C 1s high-resolution X-ray photoelectron spectra of PS16K−COOH grafted to the GPS layer before (a) and after labeling with *n*-butylamine (b): (A′ = −*C*═*C*−; A = C_xH_y; B′ = −*C*−N; C′ = −*C*−O−*C*− and −*C*−OH).

Table 3. Component Peaks of C 1s XPS for the Layer of Grafted PS−COOH and Labeled Residual Epoxy Groups with *n*-Butylamine

A 285.00 e.V	A′ 284.76 e.V	B′ 285.75 e.V	C 286.32 e.V
C_xH_y	−C═C−	−*C*−N	−*C*−O−*C*− and −*C*−OH

with different functionalities and at least two of them (hydroxy and epoxy groups) can be used for the grafting of the carboxyl-terminated polymers.

Grafting of the First Polymer. The next step of the synthetic procedure comprises the grafting of the PS−COOH from the thin film deposited on the surface of the Si wafer with chemisorbed GPS using spin-coating from 1% toluene solution. The kinetics of the grafting of PS−COOH in terms of the ellipsometric thickness of the layer is presented in Figure 5. For XPS investigations, we used the sample with 1.4 mg/m^2 grafted GPS and 4.2 mg/m^2 grafted PS−COOH. In the C 1s XPS spectrum (Figure 6), we observed a peak of −C═C− (the main component) bonds representing the aromatic phenyl ring system (284.76 eV) (the corresponding shake-up peak appears at 292 eV) of polystyrene and the second component peak shows the presence of C−O (286 eV) bonds. The FTIR-ATR spectra shown in Figure 4c provide further evidence of the grafting of PS−COOH. In the spectra, we identify very pronounced PS bands at 1601, 2923, and 3027 cm^{-1}.

We used *n*-butylamine again to label the residual epoxy groups after grafting of PS−COOH. The XPS data (Figure 6b) evidence the essential amount of epoxy functionalities. We identified the N 1s peak at 398.76 eV. The C 1s spectrum was decomposed into five component peaks named A, A′, B′, and C. The different carbon species are given in Table 3. The elemental ratio [N]/[C] determined from the decomposed C 1s spectrum according to

$$\frac{[\mathrm{N}]}{\Sigma\mathrm{carbons}} = \frac{0.5\,[\mathrm{B}']}{[\mathrm{A}'] + [\mathrm{A}] + [\mathrm{B}'] + [\mathrm{C}]} = 0.0255$$

excellently matches the value from the survey spectrum, 0.02. The labeling reaction clearly shows that the substrate surface contains accessible epoxy groups even after carrying out the first grafting of PS−COOH.

As can be seen from Table 4, the number of grafted chains of PS−COOH is much smaller than the number of functional reactive groups (hydroxyl + epoxy) on the surface even if their fraction is only 10% of total amount of chemisorbed GPS. They are in excess and do not limit grafting of the polymers. Indirect evidence for that is the experimental relationship between plateau grafting amount and molecular weight of PS−COOH (Figure 7). The obtained relationship is similar to the data presented in the literature for different chemical reactions used for the "grafting to" approach.[21,26] The plateau grafting amount is kinetically limited by chain penetration through the grafted brush and scales with the bulk radii of gyration of the polymer chains. The relationship passes through a maximum because for very large coils the probability of the contact between the end-functional group and a functionality on the substrate is very small.[21]

For synthesis of binary brushes of different compositions, it is important to regulate the grafted amount of the first grafted polymer. That can be done by a change of both grafting time and temperature. For example, for the PS72K−COOH (M_W = 75 000) after 2 h of grafting at 120, 130, 140, and 150 °C the brushlike layer thickness was 3, 4.5, 6.3, and 9 nm, respectively. The plateau grafting amount is well-reproducible parameter, while grafting kinetics shows from time to time large deviations at the initial fast stage of grafting (Figure 5).

The same investigation was performed for the grafting of the PVP−COOH spin-coated from the 1% THF solution. The ungrafted polymer was removed by Soxhlet extraction with THF. We have observed very similar grafting kinetics for both polymers (Figure 5).

Grafting of the Second Polymer. From both series of the PS−COOH and PVP−COOH grafted films, we selected samples with the film thickness smaller than the plateau value. Then the second polymer, PVP−COOH and PS−COOH, respectively, was spin-coated on top of each film, and the heating procedure followed by subsequent Soxhlet extraction to remove any ungrafted polymer was performed. Grafting of the second polymer was measured with ellipsometry (Figure 1). We observed the grafting of the second polymer only for the first case when PS−COOH was initially grafted and then PVP−COOH was grafted on the second step. For the inverse case when a PS−COOH film was deposited on top of the PVP−COOH film, we observed only few grafted PS−COOH. Consequently, this procedure is effective if the polar component is grafted after the nonpolar component. In the latter case, there is a driving force to penetrate the polymer brush of the first polymer and approach the substrate surface with residual reactive groups. The grafting of the second polymer was

(26) (a) Erb, V. Ph. D. Dissertation, Johannes Gutenberg-Universität Mainz, Germany, 1997. (b) Prucker, O.; Naumann, C. A.; Rühe, J.; Knoll, W.; Frank, C. W. *J. Am. Chem. Soc.* **1999**, *121*, 8766−8770.

Table 4. Ellipsometric Thickness (H) and Grafting Density (Σ) of Polymer Brushes after Each Step of Grafting and Adaptive Behavior of the Mixed Brushes

GPS H, nm/Σ, nm^{-2}	PS16K−COOH H, nm/Σ, nm^{-2}	PVP−COOH H, nm/Σ, nm^{-2}	advancing contact angle (deg) after exposure of the mixed brush to different solvents			
			toluene	THF	chloroform	water, pH = 3.0
1.4/4.05	3.9/0.14	3.65/0.06	84	77	72	55
1.4/4.06	5.9/0.22	1.4/0.021	85	79	76	53

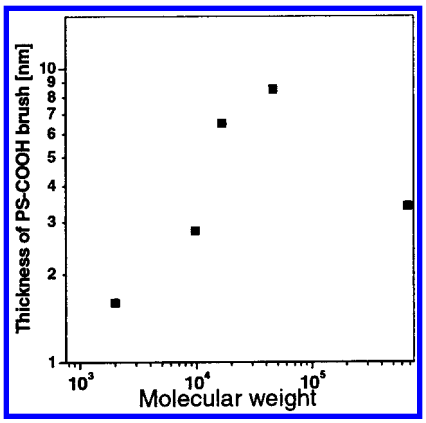

Figure 7. Influence of molecular weight of PS−COOH on the plateau thickness (dry film) of the grafted brush.

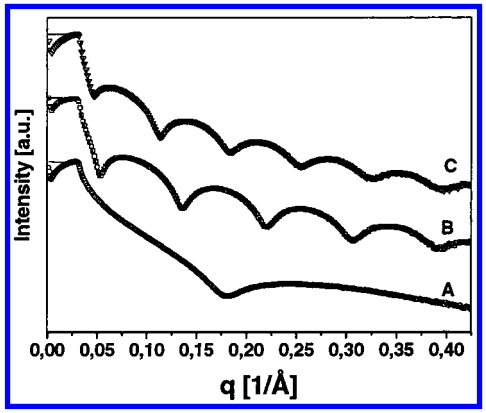

Figure 8. X-ray reflectivity curves follow the step-by-step grafting procedure: (a) chemisorbed GPS, $H = 1.7$ nm, rms = 0.42 nm; (b) grafted PS16K−COOH, $H = 5.6$ nm, rms = 0.47 nm; (c) grafted binary (PS16K/PVP) brush, $H = 7.5$ nm, rms = 0.75 nm.

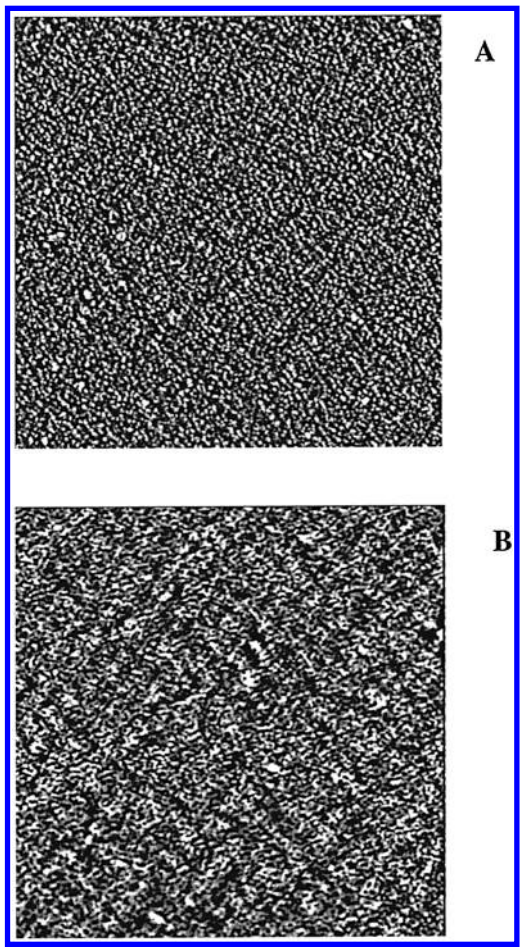

Figure 9. AFM topographical ($2 \times 2\ \mu m^2$, Z-range 5 nm) images of a PS16K/PVP binary brush after exposure to toluene rms = 0.71 nm (A) and ethanol rms = 0.92 nm (B).

proved with FTIR-ATR (Figure 4d). In addition to PS bands, we identified the characteristic bands of PVP at 1568 and 1590 cm^{-1}.

The total grafting density of both polymers is larger than 0.2 nm^{-2} (Table 4), which corresponds to the 2.3 nm average distance between grafting points. This value is smaller than the gyration radius (R_g) of grafted polymer coils (for example, for PS16K−COOH in toluene $R_g = 3.8$ nm). Consequently, the swollen polymer film can be considered as a brushlike layer.

Ellipsometric mapping shows macroscopic homogeneity of the binary brushes (Figure 1, level D). The synthesized film morphology at smaller scales was investigated with the X-ray reflectivity method (Figure 8) and AFM (Figure 9).

Both methods show that films are homogeneous and relatively smooth at the microscopic scale. This fact may be considered as an *unexpected result*. PS and PVP are strongly incompatible polymers, and we expected that the deposited PVP film might dewet the PS brush. That might induce a complicated morphology (holes, droplets, etc.)[27] and inhomogeneous grafting of PVP. Nevertheless, we did not observe some morphology which could be originated from a dewetting phenomenon for this system. In AFM images, we observe phase segregation in the mixed brushes, which occurs at a nanoscopic dimension with the apparent average lateral size of domains of about 25−70 nm. The size of the domains is overestimated because it is almost impossible for this morphology to perform the convolution procedure correctly for the tip curvature radius. We present $2 \times 2\ \mu m^2$ images to demonstrate the laterally segregated phases (Figure 9). Any other structures were observed at larger scales ($50 \times 50\ \mu m^2$). From this result, we may assume that mutual distribution of grafted points of both polymers in the grafted layer results from interplay between grafting and dewetting kinetics. Already-grafted chains may also change the wettability of the film. To prove this assumption, we present the morphology of the binary brush prepared from maleic anhydride terminated polypropylene and PVP−COOH. PP−MA was grafted on the first step (3 nm). Then after Soxhlet extraction, PVP−COOH was spin-coated on top of the layer and heated. In this case, we observe the grafted

(27) See for example: Reiter, G.; Sharma, A.; Casoli, A.; David, M. O.; Khanna, R.; Auroy, P. *Europhys. Lett.* **1999**, *46*, 512−518.

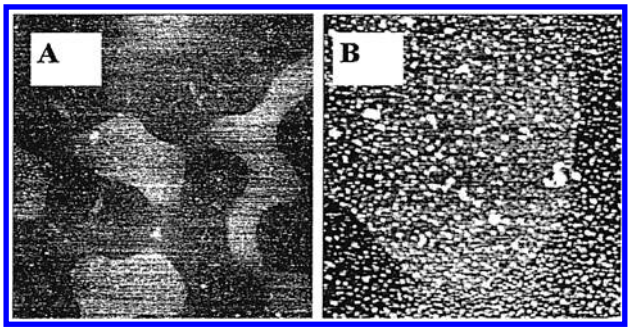

Figure 10. AFM topography images of a grafted PP−MA/PVP−COOH mixed brush showing inhomogeneous grafting at the scale 25 × 25 μm^2 and *Z*-range 25 nm (A) and 5 × 5 μm^2 and *Z*-range 10 nm (B).

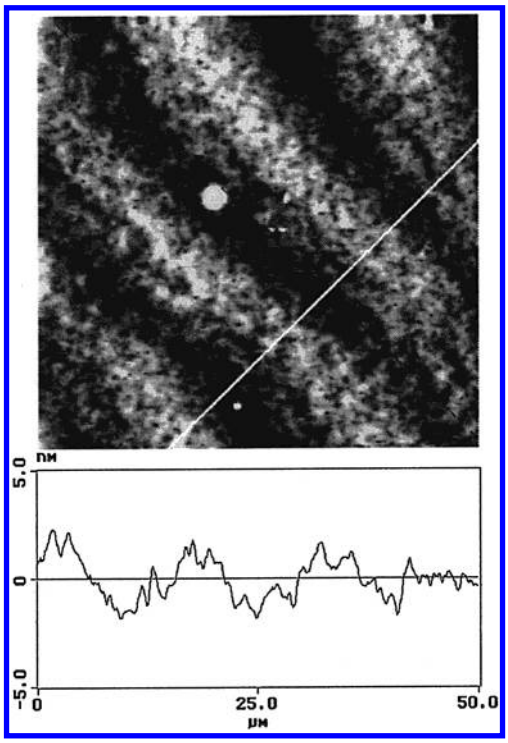

Figure 11. AFM topography image (50 × 50 μm^2) and corresponding cross section (*Z*-range in nm) of polymer film prepared by spin-coating of the mixture (1:1) of PS16K−COOH and PVP−COOH.

film morphology caused by dewetting. The AFM images at different scales (Figure 10) represent the example of the morphology formed when the dewetting process is faster than the chemical grafting. The areas with different grafting density of PVP can be recognized on the film surface.

Finally, we present as a reference the grafting experiment from the blend of polymers PS16K−COOH and PVP−COOH. Both polymers were dissolved in a common solvent (THF) and spin-coated on the Si wafer. The obtained film morphology before grafting is shown in Figure 11. After heating for 12 h and Soxhlet extraction, we found a smooth film (with AFM) with only grafted PVP (with FTIR) on the surface. Consequently, in this experiment the film deposition from the common solvent resolves film morphology with preferential location of PVP−COOH on the surface of the substrate, while PS−COOH chains occupy the top of the film. In this case, we had the same situation as in the experiment with PS−COOH deposited on the surface of the PVP brush.

Switching/Adaptive Properties. The binary brush morphology and surface energetic state switch reversibly

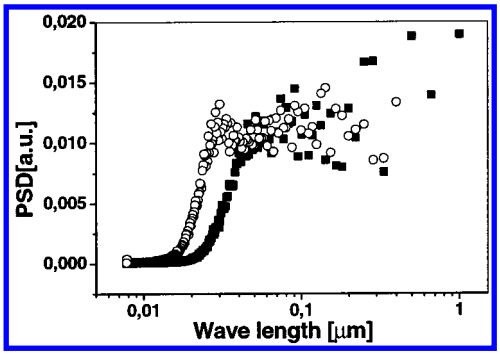

Figure 12. Radially averaged power spectra density from AFM image of the binary (PS16K/PVP = 1:1) brush upon exposure to ethanol (spheres) and toluene (squares). The peaks represent the dominant length scale.

upon exposure to different solvents in the same way as was observed for the binary brushes prepared via the "grafting from" approach.[17,18] To prove this fact, we present the data of AFM, X-ray reflectivity, and contact angle measurements for the PS/PVP (1:1) binary brush. After exposure to different solvents, the silica wafers were taken from the solvent and rapidly dried under nitrogen flux. Then the appropriate measurements of the film characteristics were performed. In these experiments, we assume that the morphology of the dry film is also characteristic for the swollen film. Time of the switching in a particular solvent is in the order of minutes, that is, larger than the time to dry the film under nitrogen flux. We may assume that we freeze the film morphology in this procedure. At ambient conditions, the polymers in the dry film are in a glassy state and the film morphology is stable for a long period of time.

Contact angles of water were measured on the surface of the wafer immediately after the drop was set on the substrate. In such experiments, we measure a contact angle on the surface of the frozen layer structure before it is changed under the water drop. Then the wafer was exposed to the next solvent and the same measurements were carried out. All changes of film properties observed experimentally are reversible, and the switching experiments were repeated several times for each sample.

AMF images show the change of morphology and roughness of the polymer films upon exposure to toluene and ethanol (Figure 9). We identified two different lateral morphologies: dimple (round clusters) after toluene and ripple (elongated domains) after ethanol. These two morphologies match very well the theoretical predictions and are caused by lateral phase segregation of two grafted incompatible polymers in the binary brush. The quantitative characteristic of the switching can be obtained in terms of the dominant length scale of the surface structure from the radially averaged power spectra density (PSD) after Fourier transform of the AFM images (Figure 12). The plots show very pronounced switching between 30 nm and 70 nm characteristic length upon exposure to toluene and ethanol, respectively.

The switching of morphology can be also seen very nicely from X-ray reflectivity curves obtained after exposure of the sample to different solvents (Figure 13) indicating the change of the film roughness (rms from 0.55 to 1.1 nm).

The switching/adaptive behavior of the binary brushes can be observed from the contact angle data (Table 4). The data clearly show that a top layer of the binary brush switches from hydrophobic to a hydrophilic energetic state upon exposure to selective solvents. When we expose the sample to toluene, the top of the layer is preferentially

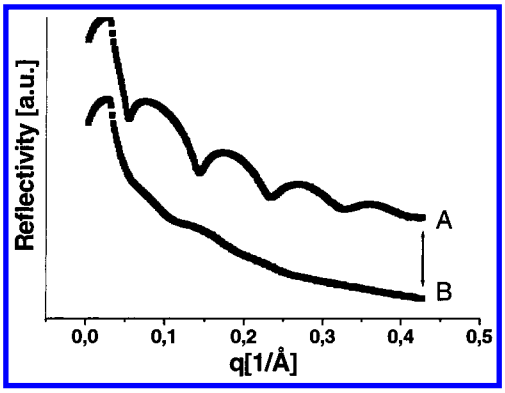

Figure 13. X-ray reflectivity curves of the binary (PS45K/PVP = 1:1, H = 5.8 nm) brush upon exposure to toluene rms = 0.5 nm (A) and ethanol rms = 1.1 nm (B).

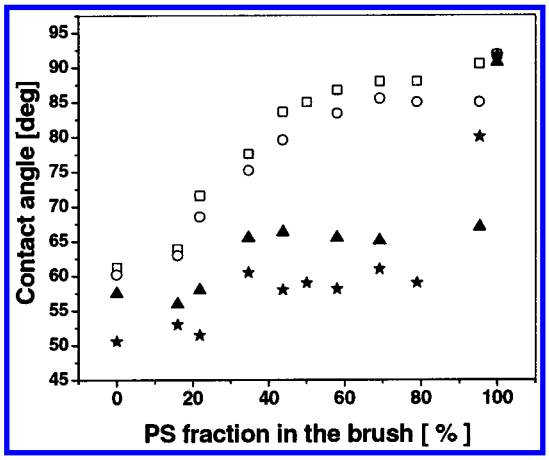

Figure 14. Switching of binary brushes (PS45K/PVP) upon exposure to water pH = 3 (stars), ethanol (triangles), THF (circles), and toluene (squares) in terms of contact angle of water vs brush composition.

occupied by PS, while in ethanol and water (pH = 3.0) the surface is dominated by PVP. In intermediate cases, after exposure to chloroform or THF, both polymers are present on the top of the film. In a broad range of the binary brush compositions, the range of switching between hydrophobic and hydrophilic states is not strongly affected by the composition (Figure 14): the brushes ranging from 10% to 90% of PS show the same hydrophilic property upon exposure to water, and those ranging from 40% to 90% of PS have the same hydrophobic properties upon exposure to toluene.

Even a small fraction of PVP can switch the brush to a hydrophilic state and vice versa. Nevertheless, the plots (Figure 14) are not symmetric with respect to the composition. We explain that by the effect of the SiO_2–substrate which acts as an additional driving force for the penetration of water through the thin polymer film.

Such a switching behavior of the binary brush suggests both lateral and perpendicular phase segregation which is considered to be a second-order transition resulting from the interplay between segment–segment and segment–solvent interactions.

Conclusions

In summary, binary adaptive polymer brushes can be easily synthesized on a Si substrate with the chemisorbed GPS via the sequential grafting of a carboxyl-terminated polystyrene on the first step and then a carboxyl-terminated poly(2-vinylpyridine) on the second step. The synthesis can be performed in any lab and does not require a special apparatus. The composition of the brush can be controlled by time and temperature of grafting in each step. The synthesized films are macroscopically homogeneous, possess phase segregation at the nanoscopic level, and show the same switching behavior as binary brushes prepared by the "grafting from" approach. The film response to the change of surroundings can be nicely detected with AFM, X-ray reflectivity, and contact angle measurements. By an appropriate choice of solvent, the binary brush can be switched from hydrophilic to hydrophobic (and vice versa) surface energetic states in the wide range of the binary brush compositions. Thus, this synthesis provides a simple method of fabrication of smart thin films for a wide variety of technical and biomaterial applications.

Acknowledgment. We are grateful for financial support of this research from Deutsche Forschungsgemeinschaft (Grants Sta 324/10-1 and Sta 324/8-1) and BMBF (Grant 05 KS1BPA/4). We thank Dr. K. Grundke, Mrs. G. Adam, and Mr. D. Pleul for providing assistance in contact angle, FTIR-ATR, and XPS spectroscopic investigations. We also thank Dr. I. Luzinov and Dr. M. Müller for stimulating discussions.

LA015637Q